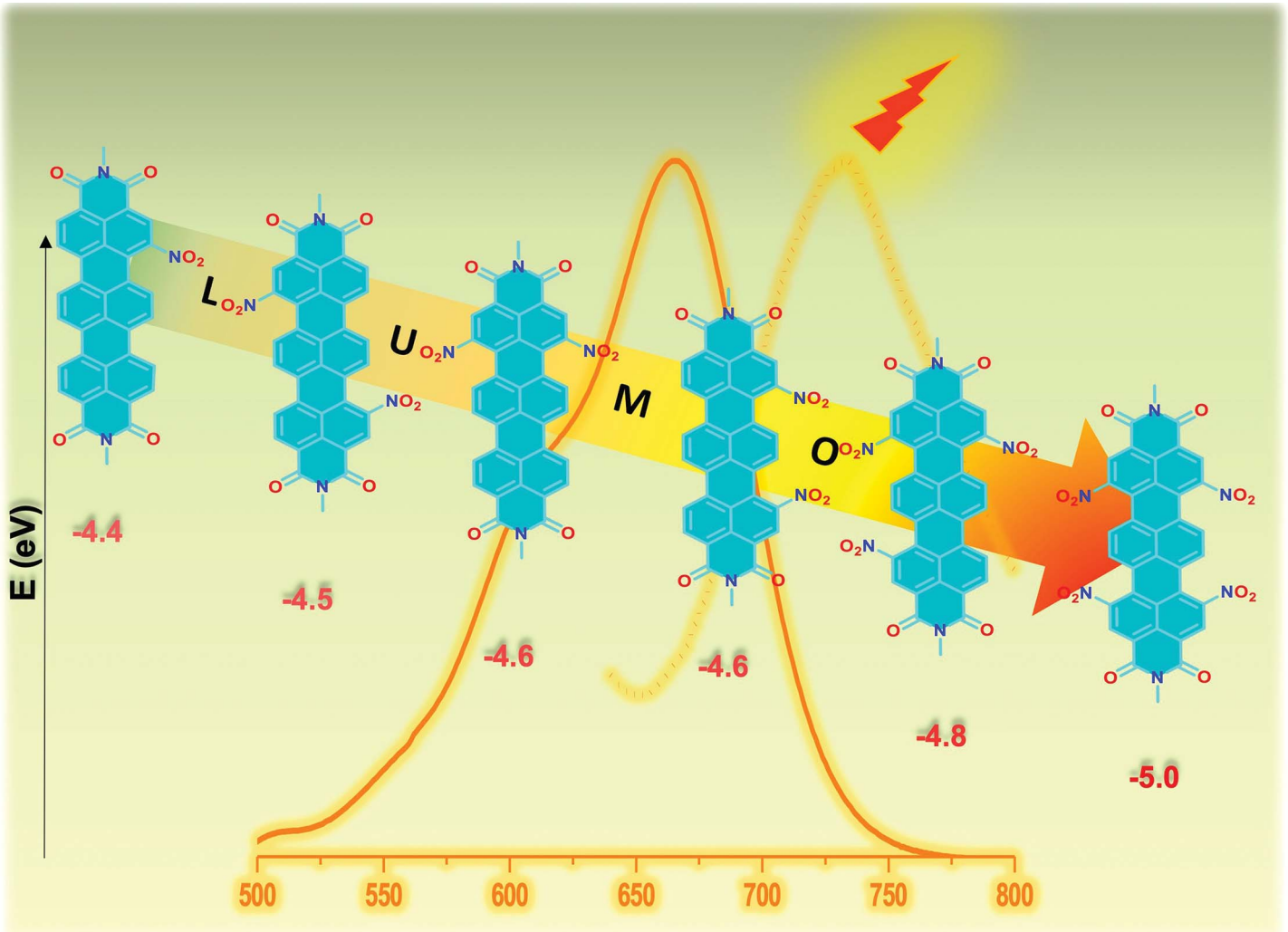

Showcasing research from Professor Jeyaraman Sankar's laboratory, Department of Chemistry, Indian Institute of Science Education and Research Bhopal, Bhopal, India.

The deeper it goes, the brighter it glows: NIR emissive nitro-terrylene diimides with deep LUMOs

Molecules with ultra-low LUMO energy levels are highly reactive and unstable under ambient conditions. Herein, we report the identification of nitrated terrylene diimides as a series of stable deep-LUMO materials. Contrary to the expectation for nitroaromatics, the molecules also fluoresce, including in the elusive near-infrared region.

As featured in:

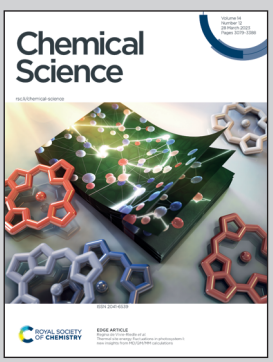

See Jeyaraman Sankar *et al.*, *Chem. Sci.*, 2023, **14**, 3147.

ROYAL SOCIETY OF CHEMISTRY

rsc.li/chemical-science

Registered charity number: 207890

Chemical Science

ROYAL SOCIETY OF CHEMISTRY

EDGE ARTICLE

View Article Online
View Journal | View Issue

Cite this: *Chem. Sci.*, 2023, **14**, 3147

All publication charges for this article have been paid for by the Royal Society of Chemistry

Received 8th November 2022
Accepted 29th January 2023

DOI: 10.1039/d2sc06162g

rsc.li/chemical-science

The deeper it goes, the brighter it glows: NIR emissive nitro-terrylene diimides with deep LUMOs†

Kundan Singh Mehra, Shivangee Jha, Anila M. Menon, Deepak Chopra and Jeyaraman Sankar *

Herein, we present the first examples of air-stable, deep-lowest unoccupied molecular orbital (LUMO) polycyclic aromatic molecules with emission in the near-infrared (NIR) region, using nitration as a strategy. Despite the fact that nitroaromatics are non-emissive, the choice of a comparatively electron-rich terrylene core proved to be beneficial for achieving fluorescence in these molecules. The extent of nitration proportionately stabilized the LUMOs. Tetra-nitrated terrylene diimide exhibited a deep-LUMO (≤−4.5 eV) of −5.0 eV *vs.* Fc/Fc$^+$, the lowest for any larger RDIs. These are also the only examples of emissive nitro-RDIs, with larger quantum yields.

Introduction

Luminescent molecules emitting in the near-IR region (NIR) find wide applications in organic light emitting diodes (OLEDs),[1] in organic solar cells,[2] and in photobiomodulation (PBM), including for side-effect alleviation after chemoradiotherapy.[3] Very few electron-deficient molecules are known to have emission in the NIR.[4] This is due to the π-extension or expansion strategy utilized for this purpose. While this method helps in reducing the band gap (E_g), most of the well-known NIR emitters such as porphyrins, phthalocyanines or squaraines, are always used as donors in optoelectronic devices.[1,5] Also, the narrow bandgap influences the stability of the molecules on prolonged use.[6] Alternatively, electron-deficient rylene diimides (RDIs) have been explored to achieve NIR absorption and emission by the π-extension approach.[7] However, this strategy could not sufficiently lower the LUMO levels, to suit their application as efficient acceptors.

Open-shell or closed-shell RDIs with electron-withdrawing substituents have classically been exploited as molecules with stabilized LUMOs (Scheme 1).[8] In this direction, tetracyanated naphthalene diimide NDI-CN$_4$ has been shown to have a deep-LUMO value of −5.0 eV *vs.* Fc/Fc$^+$. This is attributed to the smaller π-core connected to multiple electron-withdrawing units.[8a] Even though this approach helped to achieve low LUMO levels, the resultant molecule lacked any emission. On the other hand, larger RDIs such as perylene diimides (PDIs) and terrylene diimides (TDIs), despite their bathochromically shifted absorption and emission, could not lower the LUMO on simple cyanation (−4.4 eV and −4.49 eV *vs.* Fc/Fc$^+$, respectively).[9] Recently, Li *et al.* and Tan *et al.* have reported aggregation induced, emissive RDI-based molecules albeit with LUMO energies at −3.5 and −3.6 eV respectively.[10]

Deriving from the positive Hammett constants, the nitro group can be an effective alternative. However, in nitroaromatics, the preferred route of excited state relaxation is non-radiative stemming from efficient intersystem crossing. This non-emissive nature of nitroaromatics makes them less attractive despite their ability to efficiently stabilize the LUMO levels.[11]

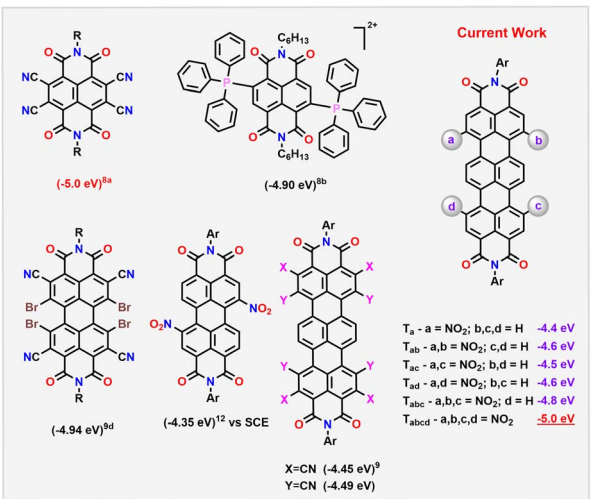

Scheme 1 Selected examples of RDIs with their LUMO levels (*vs.* Fc/Fc$^+$).

Department of Chemistry, Indian Institute of Science Education and Research (IISER) Bhopal, Bhopal Bypass Road, Bhopal, India – 462066. E-mail: sankar@iiserb.ac.in

† Electronic supplementary information (ESI) available. CCDC 2204224–2204228. For ESI and crystallographic data in CIF or other electronic format see DOI: https://doi.org/10.1039/d2sc06162g

Predictably, dinitro-PDIs with a lower LUMO level of −4.35 eV (*vs.* Saturated Calomel Electrode (SCE)) exhibited no emission.[12]

In recent years, there is a renaissance in developing novel luminescent nitroaromatics for modern optoelectronic and biomedical applications.[11] One of the exploited routes to achieve emission in these molecules is by the introduction of intramolecular donor–acceptor nature in their excited state. This charge transfer (CT) character can hinder the spin–orbit coupling (SOC), facilitating a reduced overlap between the π-orbital on the aromatic unit (donor) and the n-orbital on the nitro group (acceptor). This results in favourable radiative deactivation. Nitro-PDIs are non-emissive presumably because of the ineffective intramolecular charge transfer (ICT) between electron-deficient PDI and NO_2 units.[11,12] In this regard, a possible route could be to choose a larger RDI such as TDI.[7,13] That (i) will aid in obtaining multiple nitration on the core to achieve deeper LUMOs; (ii) will help to modulate the intramolecular charge transfer in their excited states, rendering them emissive; (iii) will also alleviate any possible steric crowding at the bay positions.

In the current work, we demonstrate that this strategy leads to the formation of a series of nitro derivatives, such as mono, di-, tri- and tetra-nitro TDIs in good yields. With the extent of nitration, their LUMO levels (*vs.* Fc/Fc^+) get stabilized proportionately from $\mathbf{T_a}$ (−4.4 eV) to $\mathbf{T_{abcd}}$ (−5.0 eV) (Scheme 1). It is to be highlighted here that $\mathbf{T_{abcd}}$ also emits in the NIR region, thus making it one of the unique electron-deficient molecules with a deep-LUMO level to do so.

Results and discussion

Synthesis

A heterocoupling reaction of perylene monoimide (PMI) with naphthalene monoimide (NMI)[7b] in the presence of sodium tertiary butoxide and 1,5-diazabicyclo(4.3.0)non-5-ene (DBN) yielded the parent TDI in 36% yield (Scheme 2). Novel nitro-TDI derivatives were obtained by careful addition of concentrated nitric acid to TDI in chloroform under ambient conditions. The extent of nitration could precisely be controlled with reaction duration and equivalence of nitric acid. Unlike the case of PDI, the reaction proceeded without the need for any additive.[12] Mono-nitrated TDI $\mathbf{T_a}$ was obtained rapidly (85%), within a few minutes of the addition of HNO_3 to TDI, along with trace amounts of dinitro-TDIs. The quick formation of $\mathbf{T_a}$ reiterates the ease of nitration of TDI. Increasing the equivalents of acid and the reaction duration (100 eq. & 1 h) yielded a complex mixture of three regioisomers of dinitro-TDIs in yields ranging from 20–40%. In contrast to bromination, all three possible regioisomers namely $\mathbf{T_{ac}}$ (1,9-) and $\mathbf{T_{ad}}$ (1,14-), including $\mathbf{T_{ab}}$ (1,6-) could successfully be obtained and characterized.[14] Incidentally, this is the first instance in which all three isomers of di-substituted TDIs have been achieved. Through this method, even tri- and tetranitro-TDIs namely $\mathbf{T_{abc}}$ and $\mathbf{T_{abcd}}$ could be obtained in moderate yields (50% and 55% respectively), without the use of any harsh or hazardous conditions. All the molecules have been isolated and purified by column chromatography using CH_2Cl_2/hexane as eluents and recrystallized from CH_2Cl_2/MeOH. The complete characterization data are provided in the ESI (Fig. S1–S24†).

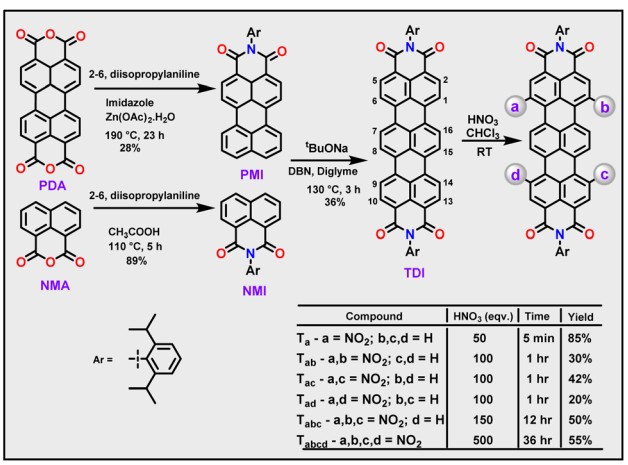

Scheme 2 Synthetic scheme for the nitration of terrylene diimides.

SCXRD studies

The structures of the molecules have been unambiguously ascertained by single crystal X-ray diffraction (SCXRD) studies. Despite our best efforts, suitable single crystals could not be obtained for $\mathbf{T_a}$. Except for $\mathbf{T_a}$, all the other nitro-TDIs afforded crystals by a solvent vapour diffusion method. The obtained structures have been given in Fig. 1. The structures of all the molecules show an almost planar TDI core, with the NO_2 groups protruding out in varying angles.

The central naphthalene rings, flanked by two NMI units, twist out of the main plane slightly. This twist was observed to be proportional to the number of NO_2 units attached to the bay region and to the positions of the NO_2 groups. In the case of $\mathbf{T_{ab}}$, the structure reveals two different conformers in the unit cell; in one of them, the two $-NO_2$ units are placed above the neighbouring naphthalene ring ($\mathbf{T_{ab}}$-*cis*), maintaining the planarity of the core. In the other conformer, the two groups are placed above and below the neighbouring ring ($\mathbf{T_{ab}}$-*trans*) as shown in the Fig. 2a inset. This suggests that in solution, this molecule is expected to have at least two conformers contributing to the photophysical properties (*vide infra*). The solid-state structure of $\mathbf{T_{ad}}$ reveals a planar TDI core, with the exception of only two C–H units of the central naphthalene pointing upwards. In $\mathbf{T_{ac}}$, both the naphthalene monoimide units twist symmetrically in opposite directions, with respect to the central naphthalene unit. As expected, $\mathbf{T_{abc}}$ assumes an unsymmetrical structure. One of the NO_2 groups in this molecule is positionally disordered between two bay positions. However, the introduction of an additional nitro group to the bay position affords a symmetrically twisted $\mathbf{T_{abcd}}$ with an angle of 19.3° between the mean plane and the central naphthalene ring.

The larger π-surface of these molecules is supposed to facilitate π–π stacking in the solid state. However, a near-perpendicular arrangement of the aryl groups on the imide

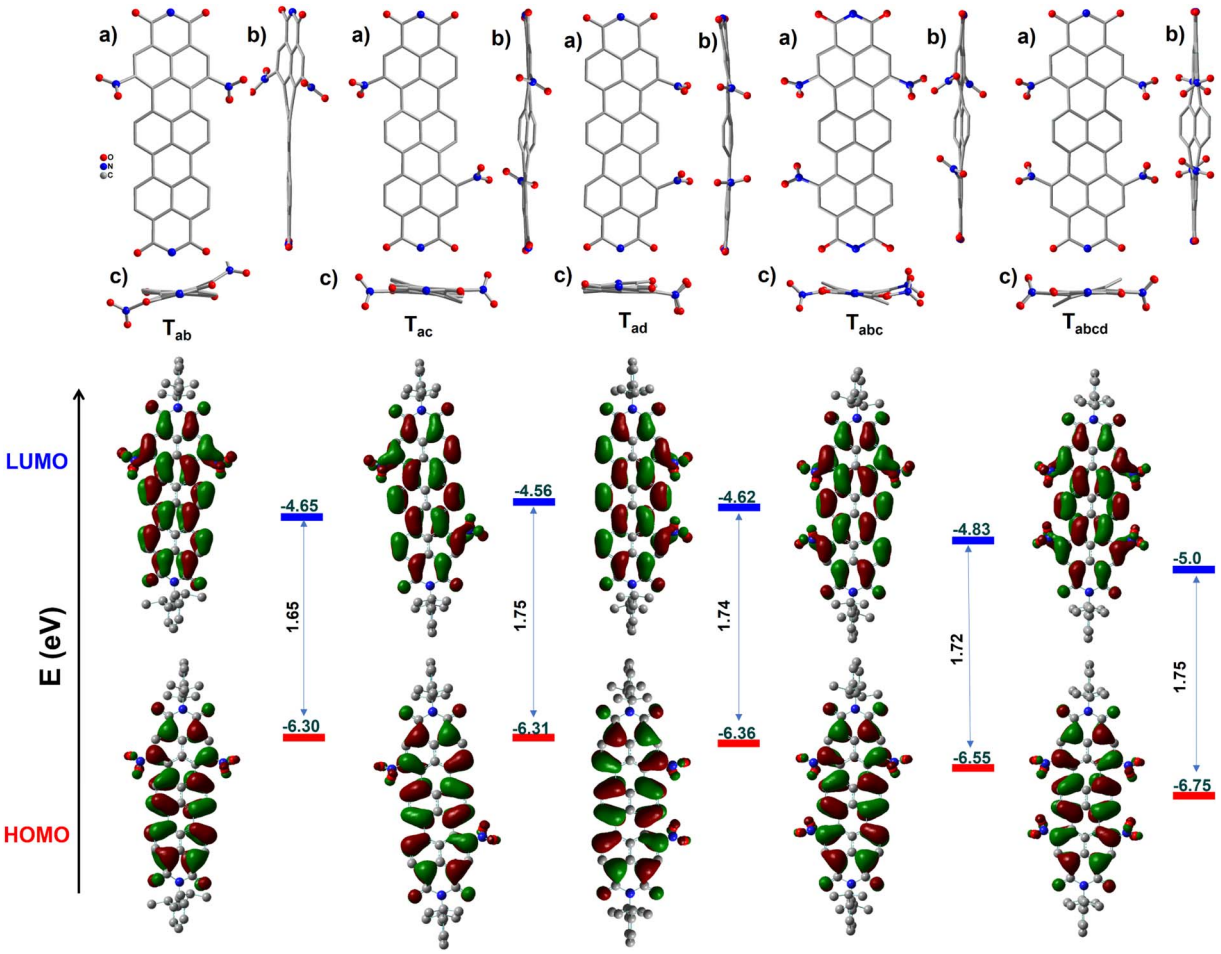

Fig. 1 Molecular structures obtained from single crystal X-ray diffraction studies (CCDC 2204224–2204228). (a) Top views, (b and c) side views, and Frontier molecular orbitals (DFT-B3LYP-6-31G**) with experimental energy levels. Hydrogen atoms and lattice solvent molecules have been removed for clarity.

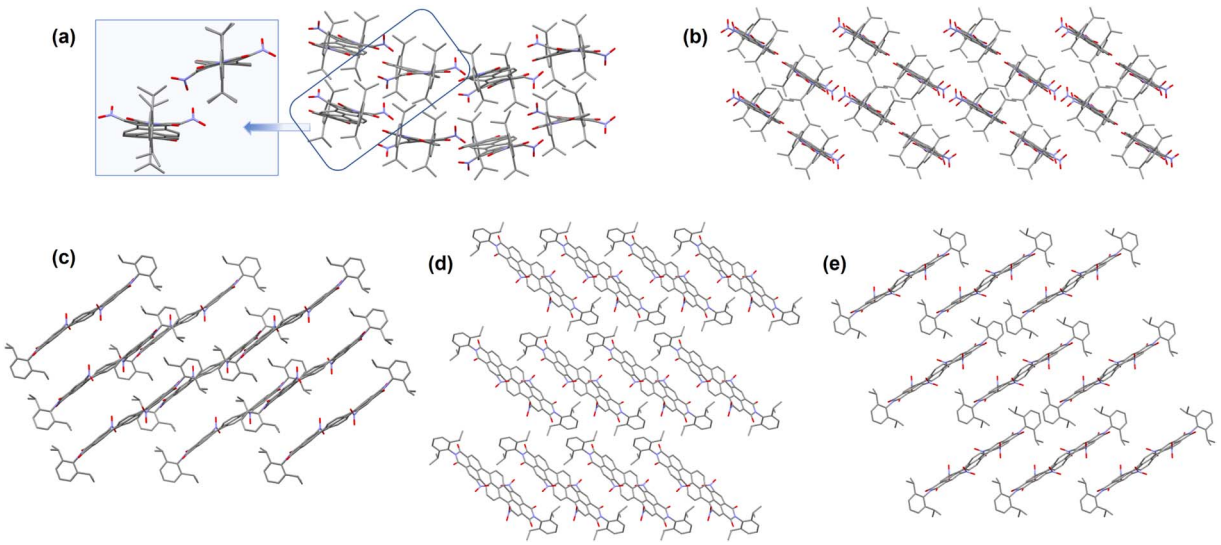

Fig. 2 Solid state packing diagrams for the nitro-TDIs, as obtained from SCXRD studies (a) T_{ab} (inset: $T_{ab\text{-}cis}$ & $T_{ab\text{-}trans}$); (b) T_{ad}; (c) T_{ac}; (d) T_{abc}; (e) T_{abcd}.

nitrogens and the NO_2 groups at the bay positions prevented strong intermolecular stacking (Fig. 2). Instead, several C–H···π contacts and C–H···O hydrogen bonds are seen in the packing of these molecules. It is presumed that this arrangement in the solid state is responsible for the ready solubility of these molecules in common organic solvents. It is seen that the lattice solvent molecules, wherever present, bind with the core of the TDI *via* C–H–π interactions and with the imide oxygens *via* C–H···O hydrogen bonding.

Cyclic voltammetry

In cyclic voltammetric studies (*vs.* Fc/Fc^+), it was observed that the first reversible reduction potentials ($E_{1/2}^{red1}$) gradually became anodic with the increase in the extent of nitration (Fig. 3a). $\mathbf{T_a}$ exhibited $E_{1/2}^{red1}$ at −0.34 V, which is significantly lower than that observed for TDI (−0.60 V). Strikingly, even the second reduction of $\mathbf{T_a}$ is easier (−0.47 V) than the first reduction of TDI (Table 1 & Fig. S36†). Only $\mathbf{T_a}$ shows a reversible oxidation wave within the potential range scanned, which is anodic to that of TDI. The dinitro regioisomers exhibited a peculiar trend with the $E_{1/2}^{red1}$ values of −0.15 V, −0.24 V, and −0.18 V for $\mathbf{T_{ab}}$, $\mathbf{T_{ac}}$ and $\mathbf{T_{ad}}$ respectively. This underscores the importance of the position of functionalization in fine tuning the electronic energy levels. $\mathbf{T_{abc}}$ and $\mathbf{T_{abcd}}$ can be more easily reduced with $E_{1/2}^{red1}$ values of 0.03 V and 0.20 V respectively. The stability of these molecules is of paramount importance to utilize them for further applications. To verify the same, $\mathbf{T_{abcd}}$ with the lowest reduction potential had been subjected to a cyclic test at 100 mVs^{-1} and found to be stable (Fig. 3b) even after 30 cycles. The LUMO values are listed in Fig. 1, Tables 1 and S1.† The trend observed for the values is $\mathbf{T_a}$ > $\mathbf{T_{ac}}$ > $\mathbf{T_{ad}}$ > $\mathbf{T_{ab}}$ > $\mathbf{T_{abc}}$ > $\mathbf{T_{abcd}}$. $\mathbf{T_{abcd}}$ (−5.0 eV) was found to have one of the deepest LUMOs reported for any stable, longer RDI.

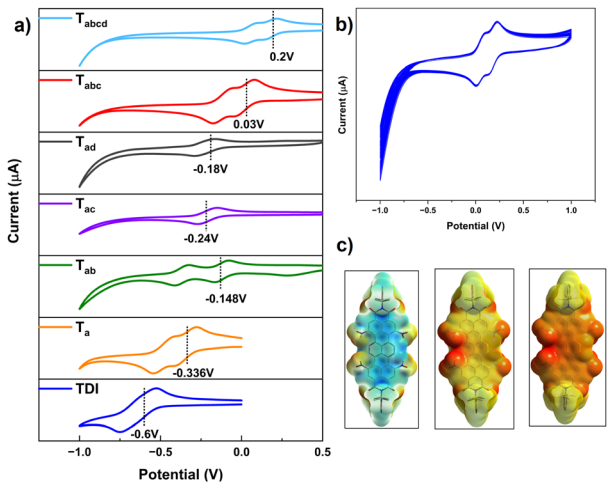

Fig. 3 Cyclic voltammograms of the nitro-TDIs *vs.* Fc/Fc^+ (a); stability of T_{abcd} after 30 cycles (b), and ESP surfaces for T_{abcd}, $T_{abcd}^{\bullet-}$, T_{abcd}^{-} (c).

Absorption and fluorescence studies

The absorption spectra of the nitrated derivatives were broader, with minimal bathochromic shifts, and less intense, compared to those of parent TDI (Table 1 & Fig. 4). This is attributed to the impending deviation of core planarity stemming from steric crowding at the bay positions.[7c,14] The di- and tetra-substituted TDIs have marginally higher molar extinction (ε) values. As found in SCXRD studies, these molecules may have other conformers in solution with improved planarity. The absorption onset obtained from the electronic spectra revealed a near identical E_g for all the nitro-TDIs, irrespective of the extent of nitration (Table 1). This is due to the stabilization of both HOMO and LUMO levels evenly.

As presumed, the nitro derivatives were found to be fluorescent. Even though the absorption profiles were in the visible region, their emission maxima were in the NIR region (>700 nm), owing to larger Stokes shifts (Fig. 4 & Table 1). Nitro-aromatics are often non-emissive in nature. They release the excitation energy effectively *via* an inter-system crossing (ISC) process. To make them emissive, it is necessary to introduce a charge transfer (CT) character in their excited states, which can be achieved by introduction of a donor-accepter configuration in the molecule. These CT states can hinder ISC and a radiative decay is preferred from the singlet states.[11a] In the present case, a comparatively electron-rich TDI forms a CT state due to the push–pull configuration with nitro groups. This in turn impedes the inter-system crossing (ISC) and facilitates a radiative channel. The emission of the nitro-TDIs stems from this phenomenon. Our hypothesis was further supported by solvent dependent emission studies. As the CT states are sensitive to solvent polarity, the effect of solvent was investigated.

Table 1 Optical and redox data for all the synthesized molecules

Comp	$\lambda_{max,abs}$ [nm]	ε [M^{-1} cm^{-1}]	$E_{g,opt}$ [eV]	$\lambda_{max,em}$ [nm]	Stokes shift [cm^{-1}]	ϕ^a [%]	E_{red} [V]	E_{ox} [V]	LUMO[b] [eV]	τ_{av} [ns]	k_r [s^{-1}]	k_{nr} [s^{-1}]
TDI	653	131 000	1.81	666	298	90	−0.60, −0.65	1.22	−4.2	3.31	2.7×10^8	3.02×10^7
$\mathbf{T_a}$	657	76 000	1.74	720	1332	3(6)	−0.336, −0.47	1.4	−4.4	1.49	2.0×10^7	6.4×10^8
$\mathbf{T_{ab}}$	669	81 000	1.65	696	580	2(2)	−0.148, −0.46	—	−4.6	1.33	1.5×10^7	7.3×10^8
$\mathbf{T_{ac}}$	658	82 000	1.75	702	952	12(14)	−0.24	—	−4.5	1.27	9.4×10^8	6.9×10^8
$\mathbf{T_{ad}}$	663	75 000	1.74	708	980	11(14)	−0.18	—	−4.6	1.38	7.9×10^7	6.4×10^8
$\mathbf{T_{abc}}$	666	68 000	1.72	732	1354	2(5)	0.03, −0.10	—	−4.8	0.98	2.0×10^7	1.0×10^9
$\mathbf{T_{abcd}}$	664	82 000	1.75	717	1113	8((10)	0.20, 0.07	—	−5.0	1.39	5.7×10^7	6.5×10^8

[a] Quantum yield recorded in hexane (values from paraffin oil in parentheses), using TDI as the reference.[15] [b] LUMO *vs.* Fc/Fc^+.

Nonpolar solvents such as *n*-hexane could not stabilize the CT state and thus the molecules exhibited emission. However, in polar solvents, the CT states get stabilized effectively and exhibited redshifted emission with reduced intensity (Fig. S25–S30†).[11] In the case of the three regio-isomers of dinitro-TDIs, the emission spectra were not identical. This can be attributed to the difference in the electronic nature of the excited states, depending on the position of the nitro groups. As discussed in the X-ray diffraction analysis, $\mathbf{T_{ab}}$, where the two nitro groups are linked to the same naphthalene unit, shows two conformers in the solid state. These conformers might have dynamic interconversion in solution, thus reducing the emission intensity significantly by nonradiative decay, compared to other regio-isomers.

The fluorescence intensity of all the molecules increased significantly at 77 K (Fig. 5a–b & S34). A similar observation was obtained from a viscous paraffin oil solution of the compounds (Fig. S25–S30†). Further, there was no apparent change in emission when recorded under deaerated conditions (Fig. S31†). The emission dependence on solvent viscosity and temperature is partially attributed to the restricted dynamics around the C–N bond. Moreover, under these conditions, the nitro groups may attain co-planarity with the aromatic core and thus enhanced emission was observed. The singlet lifetimes measured were between 1 and 2 ns, much longer than expected for nitroaromatics (sub-ps or sub-ns). The radiative decay rate of $\sim 10^8$ s^{-1} further supported the emissive nature.

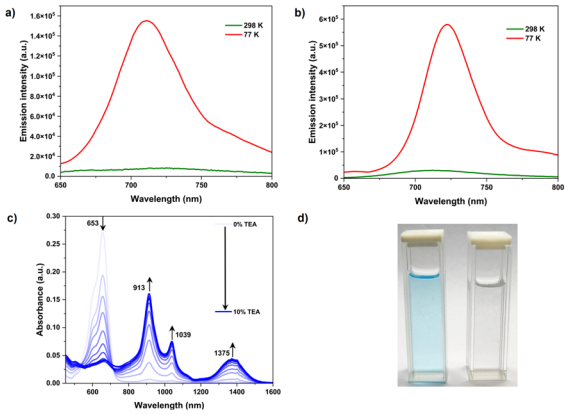

Fig. 5 Emission profiles of T_a (a) and T_{abcd} (b) at 77 K and 298 K; (c) absorption response for T_{abcd} with the addition of triethylamine in chloroform; (d) photograph of T_{abcd} before and after TEA addition.

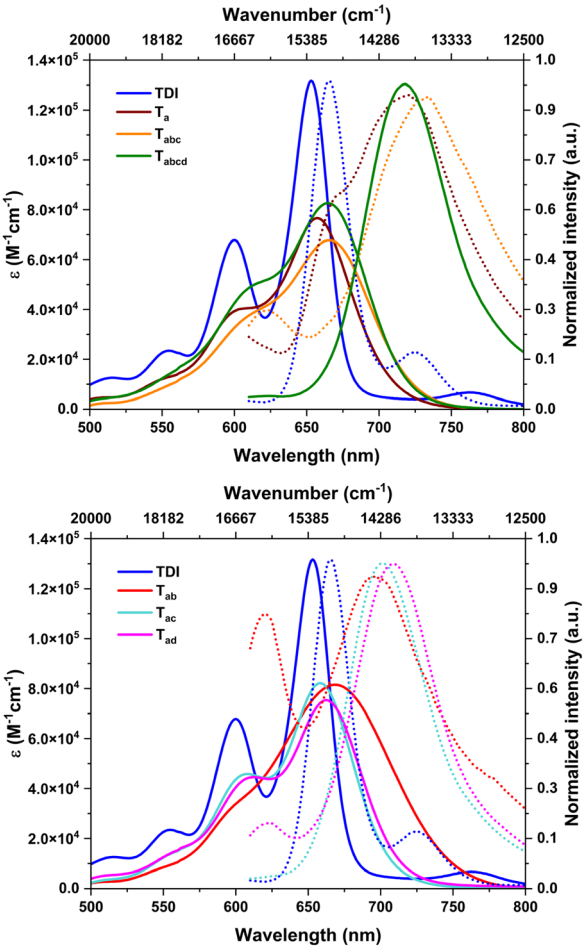

Fig. 4 Absorption (solid line) and emission spectra (dotted line) of a nitro-TDI ($\times 10^{-6}$ M) solution of $CHCl_3$ (excitation wavelength 600 nm).

The electron-deficient nature of $\mathbf{T_{abcd}}$ directs the attention towards probing its electron affinity for possible applications. The absorption spectrum obtained while titrating $\mathbf{T_{abcd}}$ in chloroform against triethyl amine exhibits a new set of bands between 900 nm and 1400 nm, with a decrease in the intensity of the 664 nm band (Fig. 5c and d). The new bands can be attributed to the formation of a dianion, even in the absence of light, reflecting the enhanced electron affinity. The direct formation of a dianion, bypassing the formation of an anion radical, can be originating from the smaller potential gap (130 mV) between the two oxidation states (Fig. 3). Further, the trend observed for the reduction of other nitro-TDIs is linearly correlated with the extent of nitration (Fig. S32†). A measure of the ease of reduction for $\mathbf{T_{abcd}}$ is further emphasized by the formation of a dianion even with a milder base such as DABCO (Fig. S33†). The easier reduction along with their strong absorption in the visible region would make them excellent catalysts.[16]

Conclusion

In summary, electron deficient derivatives of TDI with deep-LUMO energy levels have been achieved and are structurally characterized. These molecules demonstrated impressive redox stability and structural rigidity. The tunability of the redox properties of regioisomers highlights the finer flexibility in modulating the electronic nature. Its low lying LUMO enables $\mathbf{T_{abcd}}$ to get reduced even in the presence of bases such as DABCO. Owing to their apt energy levels, all derivatives showed emission in the NIR range. The fluorescence quantum yields are among the best for any electron deficient, NIR emissive molecules. This is attributed to the electronic synergy between

the TDI core and the electron withdrawing nitro groups, resulting in longer singlet lifetimes stemming from the modulation of the ICT process. The cryoemission, along with viscosity studies further support the fact that the nonradiative pathways resulting from dynamics can be suppressed to achieve intense emission. Their ultra-low LUMO levels, ambient stability, redox robustness along with emissive nature in the NIR, make nitro-TDIs excellent candidates for modern electronic applications and as catalysts. This work highlights the utility of nitration as an excellent strategy for developing new functional rylene diimides. Further investigations in these directions are currently underway.

Data availability

All necessary data have been included in the manuscript and in the ESI.†

Author contributions

K. S. M. performed all the synthesis, characterization, and experimental work. K. S. M., S. J. and J. S. analysed the data and wrote the manuscript. A. M. M. and D. C. contributed in SCXRD experiments and structure refinement. J. S. supervised the project. All authors have given approval to the final version of the manuscript.

Conflicts of interest

There are no conflicts to declare.

Acknowledgements

KSM & SJ thank CSIR, New Delhi and INSPIRE-DST, New Delhi respectively for fellowships. JS thanks DST-SERB-EMR/2016/005768 & DST-SERB-CRG/2020/004632 for funding the UV-vis-NIR spectrophotometer and semi-preparative GPC respectively. The authors thank Dr Ruchika Mishra for useful suggestions and proof-reading of the manuscript. All authors thank IISER Bhopal for infrastructure and funding.

Notes and references

1 A. Zampetti, A. Minotto and F. Cacialli, *Adv. Funct. Mater.*, 2019, 1807623.

2 (*a*) Z. Y. Wang, *Near-Infrared Organic Materials and Emerging Applications*, CRC, Boca Raton, 2013; (*b*) J. Qi, W. Qiao and Z. Y. Wang, *Chem. Rec.*, 2016, **16**, 1531–1548.

3 (*a*) F. Legouté, R. J. Bensadoun, V. Seegers, Y. Pointreau, D. Caron, P. Lang, A. Prévost, L. Martin, U. Schick, B. Morvant, O. Capitain, G. Calais and E. Jadaud, *Radiat. Oncol.*, 2019, **14**, 83; (*b*) M. A. Naeser, A. S. Marche, M. H. Krengel, M. R. Hamblin and J. A. Knight, *Photomed. Laser Surg.*, 2011, **29**(5), 351–358.

4 (*a*) M. Ito, M. Sakai, N. Ando and S. Yamaguchi, *Angew. Chem., Int. Ed.*, 2021, **60**, 21853–21859; (*b*) X. X. Zhang, H. Qi, Y. L. Liu, S. Q. Yang, P. Li, Y. Qiao, P. Y Zhang, S. H. Wen, H. l. Piao and K. L Han, *Chem. Sci.*, 2020, **11**, 11205–11213.

5 (*a*) A. Tsuda and A. Osuka, *Science*, 2001, **293**, 79–82; (*b*) K. R. Graham, Y. Yang, J. R. Sommer, A. H. Shelton, K. S. Schanze, J. Xue and J. R. Reynold, *Chem. Mater.*, 2011, **23**, 5305–5312; (*c*) E. J. Peterson, W. Qi, I. N. Stanton, P. Zhang and M. J. Therien, *Chem. Sci.*, 2020, **11**, 8095–8104.

6 P. Cheng and X. Zhan, *Chem. Soc. Rev.*, 2016, **45**, 2544–2582.

7 (*a*) F. Holtrup, G. Müller, H. Quante, S. de Feyter, F. C. De Schryver and K. Müllen, *Chem.–Eur. J.*, 1997, **3**, 219–225; (*b*) F. Nolde, J. Qu, C. Kohl, N. G. Pschirer, E. Reuther and K. Müllen, *Chem.–Eur. J.*, 2005, **11**, 3959–3967; (*c*) K. Peneva, G. Mihov, F. Nolde, S. Rocha, J. i. Hotta, K. Braeckmans, J. Hofkens, H. U. i, A. Herrmann and K. Müllen, *Angew. Chem., Int. Ed.*, 2008, **47**, 3372–3375; (*d*) K. S. Mehra, S. Jha, S. Bhandary, D. Mandal, R. Mishra and J. Sankar, *Angew. Chem., Int. Ed.*, 2022, **61**, e202205600.

8 (*a*) Y. Kumar, S. Kumar, K. Mandal and P. Mukhopadhyay, *Angew. Chem., Int. Ed.*, 2018, **57**, 16318–16322; (*b*) S. Kumar, M. R. Ajayakumar, G. Hundal and P. Mukhopadhyay, *J. Am. Chem. Soc.*, 2014, **136**, 12004–12010; (*c*) S. Kumar, J. Shukla, Y. Kumar and P. Mukhopadhyay, *Org. Chem. Front.*, 2018, **5**, 2254–2276.

9 (*a*) G. Battagliarin, Y. Zhao, C. Li and K. Müllen, *Org. Lett.*, 2011, **13**, 3399–3401; (*b*) G. Battagliarin, S. R. Puniredd, S. Stappert, W. Zajaczkowski, S. Wang, C. Li, W. Pisula and K. Müllen, *Adv. Funct. Mater.*, 2014, **24**, 7530–7537; (*c*) J. Gao, C. Xiao, W. Jiang and Z. Wang, *Org. Lett.*, 2014, **16**, 394–397; (*d*) Y. Kumar, S. Kumar, D. Bansal and P. Mukhopadhyay, *Org. Lett.*, 2019, **21**, 2185–2188.

10 (*a*) X. Sun, M.-Y. Liao, X. Yu, Y.-S. Wu, C. Zhong, C.-C. Chueh, Z. Li and Z. Li, *Chem. Sci.*, 2022, **13**, 996–1002; (*b*) D. Guo, L. Li, X. Zhu, M. Heeney, J. Li, L. Dong, Q. Yu, Z. Gan, X. Gu and L. Tan, *Sci. China: Chem.*, 2020, **63**, 1198.

11 (*a*) Y. M. Poronik, B. Sadowski, K. Szychta, F. H. Quina, V. I. Vullev and D. T. Gryko, *J. Mater. Chem. C*, 2022, **10**, 2870–2904; (*b*) C. Hansch, A. Leo and R. W. Taft, *Chem. Rev.*, 1991, **91**, 165–195; (*c*) M. C. Chen, D. G. Chen and P. T. Chou, *ChemPlusChem*, 2021, **86**, 11–27; (*d*) W. R. Córdoba, L. G. Arzaluz, F. C. Guzmán and J. Peon, *Chem. Commun.*, 2021, **57**, 12218–12235; (*e*) K. Skonieczny, I. Papadopoulos, D. Thiel, K. Gutkowski, P. Haines, P. M. McCosker, A. D. Laurent, P. A. Keller, T. Clark, D. Jacquemin, D. M. Guldi and D. T. Gryko, *Angew. Chem., Int. Ed.*, 2020, **59**, 16104–16113.

12 (*a*) K. Y. Chen and T. J. Chow, *Tetrahedron Lett.*, 2010, **51**, 5959–5963; (*b*) H. Y. Tsai, C. W. Chang and K. Y. Chen, *Tetrahedron Lett.*, 2014, **55**, 884–888.

13 (*a*) K. Lee, Y. Zu, A. Herrmann, Y. Geerts, K. Müllen and A. J. Bard, *J. Am. Chem. Soc.*, 1999, **121**, 3513–3520; (*b*) Z. An, S. A. Odom, R. F. Kelley, C. Huang, X. Zhang, S. Barlow, L. A. Padilha, J. Fu, S. Webster, D. J. Hagan, E. W. Stryland, M. R. Wasielewski and S. R. Marder, *J. Phys. Chem. A*, 2009, **113**, 5585–5593.

14 S. Jha, K. S. Mehra, A. Hasija, D. Chopra, R. Regar and J. Sankar, *J. Org. Chem.*, 2022, **87**, 3770–3774.

15 (*a*) M. Davies, C. Jung, P. Wallis, T. Schnitzler, C. Li, K. Müllen and C. Bräuchle, *ChemPhysChem*, 2011, **12**, 1588–1595; (*b*) H. Langhals, A. Walter, E. Rosenbaum and L. B. A. Johansson, *Phys. Chem. Chem. Phys.*, 2011, **13**, 11055–11059.

16 (*a*) I. Ghosh, T. Ghosh, J. I. Bardagi and B. König, *Science*, 2014, **346**, 725–728; (*b*) A. Ruffoni, C. Hampton, M. Simonetti and D. Leonori, *Nature*, 2022, **160**, 81–86.